



## Core-Shell SiO<sub>2</sub>@LDHs with Tuneable Size, Composition and Morphology

Journal:	<i>ChemComm</i>
Manuscript ID:	CC-COM-12-2014-010008.R1
Article Type:	Communication
Date Submitted by the Author:	13-Jan-2015
Complete List of Authors:	Chen, Chunping; Oxford University, Chemistry Research Laboratory Felton, Ryan; Oxford University, Chemistry Research Laboratory Buffet, Jean-Charles; Oxford University, Chemistry Research Laboratory OHare, Dermot; Oxford University, Chemistry Research Laboratory

## COMMUNICATION

## Core-Shell SiO<sub>2</sub>@LDHs with Tuneable Size, Composition and Morphology

Cite this: DOI: 10.1039/x0xx00000x

Chunping Chen, Ryan Felton, Jean-Charles Buffet and Dermot O'Hare\*

Received 00th November 2014,  
Accepted 00th November 2014

DOI: 10.1039/x0xx00000x

www.rsc.org/

**We present here a simple method for the synthesis of core-shell SiO<sub>2</sub>@LDH (LDH: layered double hydroxide) particles using an *in situ* co-precipitation without any pretreatment. The LDH composition, the overall particle size and morphology can be tuned giving now opportunities for the development of novel sorbents and catalyst systems.**

Layered double hydroxides (LDHs), also called anionic clays, are a family of compounds containing brucite-like layers and exchangeable anionic interlayers. They can be expressed with a general chemical composition  $[M_{1-x}M'_x(OH)_2]^{y+}[A^{n-}]_{y/n} \cdot zH_2O$ , where typically M is a divalent metal, M' is a trivalent cation and A is the interlayer anion.<sup>1</sup> LDHs have captured much attention in recent years due to their impact across a range of applications such as catalysis,<sup>2</sup> optics,<sup>3</sup> medical science,<sup>4</sup> and inorganic-organic nanocomposites.<sup>5</sup> However, the LDH synthesised by traditional methods normally exhibit poor morphology with serious platelet aggregation by *ab*-face stacking upon drying. This significantly hampers their potential for exploitation and practical application. Recently, we have invented a simple and effective method to produce a new generation of highly dispersible, high surface area LDHs, we have designated them as AMO-LDHs (AMO = aqueous miscible organic). AMO-LDHs have the unique chemical composition of  $[M^{2+}_{1-x}M'^{3+}_x(OH)_2]^{y+}(A^{n-})_{a/n} \cdot bH_2O \cdot c(AMO\text{-solvent})$ .<sup>6</sup> AMO-LDHs powders synthesised by this method are highly dispersed with surface areas in excess of 400 m<sup>2</sup>/g, which are nearly two orders of magnitude higher than conventional LDHs.<sup>7</sup>

The fabrication of LDH building-blocks vertically on the nano-support is another promising strategy to avoid the *ab*-face stacking aggregation. To date, many researchers have attempted to obtain such hierarchical core-shell LDH materials, using SiO<sub>2</sub> in particular. So far, there are two main approaches reported for hierarchical SiO<sub>2</sub>@LDHs. One example is using the layer-by-layer (10 times) deposition process followed by *in situ* growth technique developed by Shao *et al.*<sup>8,9</sup> Using this approach the morphology of SiO<sub>2</sub>@LDH particles could be changed from core-shell, yolk-shell to hollow shell, which results in samples which have

N<sub>2</sub> Brunauer-Emmett-Teller (BET) surface areas of 42, 68 and 124 m<sup>2</sup>/g, respectively.<sup>8</sup> In 2013, Chen *et al* reported a simpler method by using an *in situ* growth technique without any silica pretreatment. After 3 h of ultrasound treatment, monodispersed core-shell SiO<sub>2</sub>@LDH was obtained.<sup>10</sup>

Herein, we report a facile method of making SiO<sub>2</sub>@LDH microspheres without layer-by-layer deposition or ultrasound treatment. The composition of LDH as well as the thickness of LDH layer can be tuned by varying the Mg:Al ratio of the synthesis solution. The size of SiO<sub>2</sub>@LDH particles can be varied from 500 to 1200 nm. The morphological architecture of these particles can be controlled from solid core-shell, yolk-shell to hollow-shell by adjusting the pH and temperature of the synthesis.

The SiO<sub>2</sub> spheres in this work were prepared by a modified literature procedures.<sup>10,11</sup> The transmission electronic microscopy (TEM) images of the synthesised SiO<sub>2</sub> spheres with different sizes are shown in Fig. 1. The silica particles have a uniform spherical shape and are monodisperse. The size of SiO<sub>2</sub> spheres can be controlled from 268 ± 23 nm (Fig. 1a) to 816 ± 30 nm (Fig. 1c).

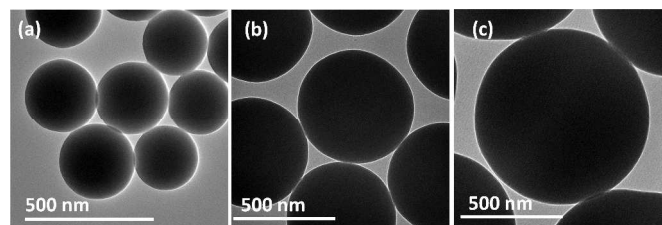


**Fig. 1** TEM images of different sizes SiO<sub>2</sub> spheres; (a) 268 ± 23 nm, (b) 499 ± 26 nm and (c) 816 ± 30 nm.

It is well known that the isoelectric point of silica particles is around 2-3.<sup>12</sup> These particles carry a high negative charge in aqueous solutions above pH 7<sup>10</sup>, this provides an excellent substrate for positively-charged LDH precursors to be electrostatically attracted to the silica surface. In this work, we have used the *in situ* co-precipitation method to directly

deposit LDH precursors on the surface of silica spheres without any binder. We observe that after aging for 3 h followed by washing at room temperature, the LDH building-blocks have grown on the silica spheres. As shown in Fig. 2, LDH nanosheets are very well oriented with the *c*-axis (LDH platelet stacking direction) tangential to the surface of the silica spheres to form a highly open hierarchical structure. We also found that the LDH platelets can be easily formed on differently sized silica spheres using the same method (Fig. 2 a-c).

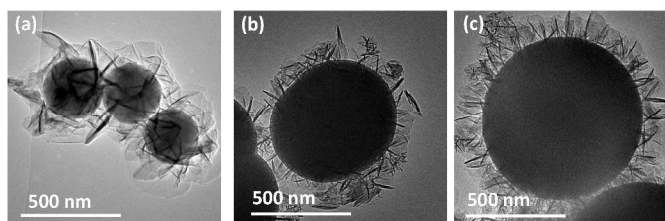


**Fig. 2** TEM images of SiO<sub>2</sub>@LDH with different size core SiO<sub>2</sub> spheres; (a) 268 ± 23 nm, (b) 499 ± 6 nm and (c) 816 ± 30 nm. (Synthesis conditions: pH 10, room temperature, Mg/Al 2:1)

The powder X-ray diffraction (XRD) patterns of the SiO<sub>2</sub> spheres, the LDH nanosheets and the SiO<sub>2</sub>@LDH hybrid particles are shown in Fig. 3a. The XRD data in Fig. 3a (i) indicate that the silica spheres all have a common amorphous structure, Fig. 3a (ii) shows the characteristic Bragg reflections of an LDHs synthesised by co-precipitation (consisting of typical layer features with a series of (00*l*) and (110) and (113) Bragg reflections). After *in situ* growth of the LDH nanosheets on the silica spheres, the XRD of the SiO<sub>2</sub>@LDH exhibits features that are a combination of both silica and the LDH. Supplementary information can also be obtained from the thermal gravimetric analysis (TGA) data (Fig. S1), where the SiO<sub>2</sub>@LDH material (Fig. S1 (b)) exhibits three typical weight losses of LDH in the range of 30 - 800 °C.

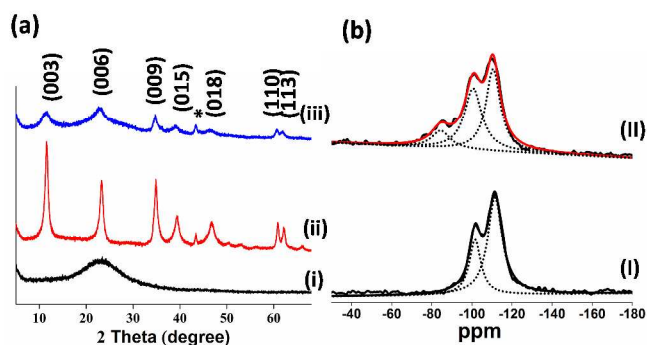


**Fig. 3** (a) XRD pattern of (i) SiO<sub>2</sub> spheres, (ii) LDH nanosheets and (iii) SiO<sub>2</sub>@LDH; (b) <sup>29</sup>Si Solid-state NMR of (I) SiO<sub>2</sub> spheres (II) SiO<sub>2</sub>@LDH particles (Synthesis conditions: pH 10, room temperature, Mg/Al 2:1, silica particle of 499 ± 25.9 nm). \* is the diffraction peak from holder.

However, neither the XRD nor the TGA data can prove that the LDH is directly connected to the silica core. <sup>29</sup>Si solid state magic-angle spinning nuclear magnetic resonance (MAS NMR) was recorded on these samples in order to probe the silicon environments in these samples. The <sup>29</sup>Si solid-state NMR spectra (Fig. 3b (I)) from the SiO<sub>2</sub> sample shows a broad resonance between -80 to -125 ppm, which can be deconvoluted into two resonances centred at -101 and -110 ppm, due to Q<sup>3</sup> (SiO)<sub>3</sub>SiOH and Q<sup>4</sup> (SiO)<sub>4</sub>Si species, respectively.<sup>13, 14</sup> The

SiO<sub>2</sub>@LDH sample (Fig. 3b (II)) shows a similar <sup>29</sup>Si solid state NMR spectrum. However, this signal can be deconvoluted into three resonances centred at -85, -101 and -111 ppm, respectively. The introduction of an extra resonance at -85 ppm is due to the formation of Si-O-Al bonds which can be a combination of Q<sup>4</sup> Si(2Al), Q<sup>3</sup> (SiO)<sub>2</sub>(AlO)SiOH and Q<sup>2</sup> (SiO)<sub>2</sub>Si(OH)<sub>2</sub>, respectively, as well as overlapping with the previously mentioned resonances of Q<sup>3</sup> (SiO)<sub>3</sub>SiOH.<sup>14</sup> The detailed information is summarised in the table S1. These findings suggest that the formation of LDH nanosheets on the surface of the silica spheres is not only as a result of electrostatic interactions but also due to the formation of Al-O-Si covalent linkages.

Using the same reaction conditions (room temperature, pH 10 and silica of 499 ± 26 nm) but varying the ratio of Mg:Al, different SiO<sub>2</sub>@LDH samples with varied compositions were obtained. Fig. S2 shows that the XRD patterns of SiO<sub>2</sub>@LDH with varying ratios of Mg:Al. Both SiO<sub>2</sub>@LDHs with Mg/Al 1:1 and 3:1 exhibit characteristic diffractions of LDH as previous mentioned, suggesting LDH with different ratios of Mg/Al can be formed in the samples using this method. The Mg:Al ratios in the SiO<sub>2</sub>@LDH was confirmed by scanning electron microscopy combined with energy dispersive X-ray spectroscopy (SEM-EDX) as shown in Table S2. The TEM images of the three SiO<sub>2</sub>@LDHs are shown in Fig. 4. The images clearly show the formed LDH nanosheets grew vertically from the surface of the silica spheres. Additionally, it is interesting to observe that the thickness of LDH layer increases with increasing Mg/Al ratio. As shown in Fig. 4a, the LDH consists of 30 - 65 nm nanosheets are attached to the silica spheres forming a uniform layer when Mg:Al ratio is 1:1. However, when the ratio increases to 3:1, a larger and denser LDH layer with the thickness of around 160 nm was formed on the surface as shown in Fig. 4c.

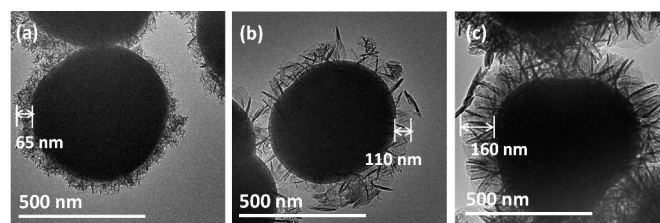


**Fig. 4** TEM images of SiO<sub>2</sub>@LDH prepared using different Mg:Al ratios; (a) 1:1, (b) 2:1 and (c) 3:1. Synthesis conditions: pH 10, room temperature, silica particle of 499 ± 25.9 nm.

Besides the flexible sizes and compositions, we found that the morphologies or architecture of the SiO<sub>2</sub>@LDH particles can also be easily tuned. Fig. 5 shows that these core@shell structures can be changed from solid core-shell (Fig. 5a), to yolk-shell (Fig. 5b) and finally to hollow-shell (Fig. 5c). We found that the pH and the temperature of the synthesis solution are the two key factors that control which structure is obtained. When the pH is too low (pH 9, room temperature) very few LDH nanosheets could grow on the surface of SiO<sub>2</sub> (Fig. S3). This is probably due to a low nucleation rate for LDH precipitation and a lower negative charge on the SiO<sub>2</sub> particles at pH 9.<sup>15</sup> When the pH was increased to 10, at room temperature, we clearly observe that a uniform layer of LDH nanosheets homogeneously grows from the surface of the silica spheres (Fig. 3b). The thickness of LDH layers is around 110 nm. Increasing the pH to 11, at 40 °C, results in

the formation of hollow-shell structures (Fig. 5a), due to the dissolution of the silica core. A similar phenomenon can be found with increasing the synthesis temperature. As shown in the Fig. 5b, the yolk-shell structure was formed with a hollow space in between the small silica core and LDH shell when 40 °C was applied at pH 10. This suggests that the interface shell between both LDH and silica is more stable than the silica in the core.

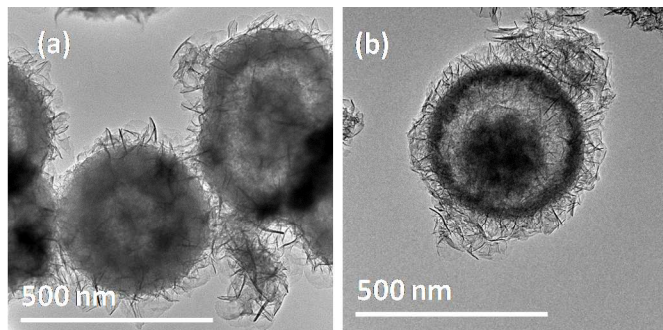


**Fig. 5** TEM images of SiO<sub>2</sub>@LDH with an Mg:Al ratio of 2:1 synthesised at : (a) pH 11 and 40 °C, Hollow-shell SiO<sub>2</sub>@LDH and (b) pH 10 and 40 °C, Yolk-shell SiO<sub>2</sub>@LDH; The SiO<sub>2</sub> particle size is 499 ± 25.9 nm

Fig. 6 shows the solid state NMR spectra of solid core-shell and yolk-shell SiO<sub>2</sub>@LDH synthesised at room temperature and 40 °C respectively. Both samples exhibit similar resonances in the <sup>29</sup>Si NMR at -85, -101 and -111 ppm, corresponding to the Si-O-Al, Si-O-H or Si-O-Si bonds (Fig. 6a). However, the yolk-shell SiO<sub>2</sub>@LDH prepared at 40 °C demonstrated a higher proportion of Si-O-Al and Si-O-H environments. As shown in the Table S3, the ratio of both the Si-O-Al and Si-O-H bonds present increased from around 33% to 45% when the samples changed from solid core-shell to yolk-shell. Moreover, the yolk-shell SiO<sub>2</sub>@LDH exhibits a broader resonance in the range 85-120 ppm, indicating that the yolk-shell SiO<sub>2</sub>@LDH sample has a different degree of Si/Al substitution including the ratio of Q<sup>4</sup> Si(1Al), Q<sup>4</sup> Si(2Al) and Q<sup>4</sup> Si(3Al).<sup>16</sup> The solid state <sup>27</sup>Al MAS NMR spectra of both SiO<sub>2</sub>@LDH samples are shown in Fig. 6b. The resonance at 10 ppm is indicative of octahedral Al sites, which are derived from the LDH structure.<sup>17</sup> However, an additional resonance at 60 ppm was found in both samples. This is attributed to tetrahedral Al sites<sup>18</sup>, indicating that during the growth of LDH on the silica surface, tetrahedral aluminium species migrate to the silicate forming Si-O-Al links. In alkali these links are more favoured compared to Si-O-Si links,<sup>19</sup> which leads to the dissolution of silica from the core and the formation of yolk-shell or hollow-shell at certain pH and temperature conditions. In comparison to the solid SiO<sub>2</sub>@LDH sample, the yolk-shell sample has a more intense <sup>27</sup>Al resonance at 60 ppm. This could be attributed to the formation of multi Si-O-Al bonding at higher temperature, which is consistent with the broad resonance observed in the <sup>29</sup>Si NMR as previously mentioned.

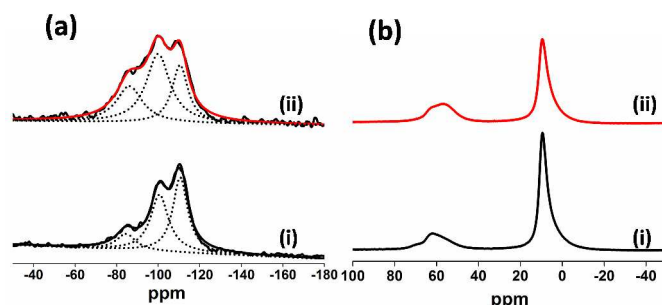


**Fig. 6** Solid state NMR spectra of SiO<sub>2</sub>@LDH synthesised at pH 10; (a) <sup>29</sup>Si MAS (b) <sup>27</sup>Al MAS. (i) Solid core-shell SiO<sub>2</sub>@LDH (pH 10 and room temperature); (ii) Yolk-shell SiO<sub>2</sub>@LDH (pH 10 and 40 °C). The SiO<sub>2</sub> particle size is 499 ± 25.9 nm

The surface areas of the SiO<sub>2</sub>@LDH's were determined by the BET method using the N<sub>2</sub> adsorption and desorption isotherms. The results are summarised in Table S4. The silica core spheres have a very low surface area of 17 m<sup>2</sup>/g. After coating the silica core spheres at room temperature with an ordered LDH layer at pH 10, the surface area increases dramatically to 107 m<sup>2</sup>/g. It is important to note that this value is significantly higher than that typical pure LDH sample (11 m<sup>2</sup>/g), indicating that this method is able to produce an LDH platelet arrangement with open hierarchical structure can effectively avoid the *ab*-face aggregation and increase surface area. If the synthesis temperature is increased to 40 °C, the obtained sample exhibits an even higher surface area of 118 m<sup>2</sup>/g, which can be explained by the introduction of more accessible void space in the yolk-shell structure as shown in Fig 5b. The surface area of the SiO<sub>2</sub>@LDH samples can be further increased by using a higher pH and temperature to obtain a hollow core structure that has a surface area of 177 m<sup>2</sup>/g. In addition, the pore size distribution of all the SiO<sub>2</sub>@LDH samples (Fig. S4) show pores in the range of 3-5 nm, 15-40 nm and 110-130 nm. An additional pore distribution in the range of 50-80 nm is observed for the yolk-shell and hollow-shell samples. This can be ascribed to the additional space inside the shell, which is evidenced by TEM and surface area as previous mentioned.

In conclusion, a simple, effective and versatile method has been developed for the synthesis of core-shell SiO<sub>2</sub>@LDH hierarchical spheres. We find that the formation of the LDH coating on the surface of SiO<sub>2</sub> is not only due to electrostatic interaction but also to the formation of Si-O-Al covalent links from the LDH layers to the SiO<sub>2</sub> core. Using this method, LDH were grown on different sized SiO<sub>2</sub> spheres from 268 – 816 nm. Furthermore, the thickness of the LDH layers can be controlled from 65 to 160 nm by changing the Mg:Al from 1:1 to 3:1, respectively. The architecture of these SiO<sub>2</sub>@LDH materials can be tuned from a solid core-shell, to a yolk-shell and finally to a hollow-shell structure. These materials exhibit a hierarchy of surface areas from 107 to 177 m<sup>2</sup>/g. We expect that the method presented in this work will open to the way to the development of wide range of new hierarchical LDH core shell materials.

C. Chen, J.-C. Buffet would like to thank SCG Chemicals Ltd, Thailand, for funding and Dr. N. Rees (University of Oxford) for solid state NMR spectroscopy.

## Notes and references

Chemistry Research laboratory, 12 Mansfield Road, OX1 3TA Oxford, UK. E-mail: Dermot.ohare@chem.ox.ac.uk

Electronic Supplementary Information (ESI) available: [Detailed experimental and characterization, X-ray powder crystallography, thermal gravimetric analysis, transmission electronic microscopy, scanning electron microscopy combined with energy dispersive X-ray spectroscopy, NMR analysis, N<sub>2</sub> Brunauer-Emmett-Teller (BET) measurement and pore size distribution]. See DOI: 10.1039/b000000x/

19. J. C. Groen, L. A. A. Peffer, J. A. Moulijn and J. Pérez-Ramírez, *Colloids and Surfaces A: Physicochem. Eng. Aspects*, 2004, **241**, 53-58; M. Ogura, S.-y. Shinomiya, J. Tateno, Y. Nara, M. Nomura, E. Kikuchi and M. Matsukata, *Appl. Catal. A*, 2001, **219**, 33-43.

1. V. Rives, *layered double hydroxides: present and future*, Nova Science Publishers, 2001; X. Duan and D. G. Evans, *Layered double hydroxides*, Springer Verlag, 2006; F. Cavani, F. Trifiro and A. Vaccari, *Catal. Today*, 1991, **11**, 173-301.
2. F. Song and X. Hu, *Nat. Commun.*, 2014, **5**; Y. Zhao, B. Li, Q. Wang, W. Gao, C. J. Wang, M. Wei, D. G. Evans, X. Duan and D. O'Hare, *Chem. Sci.*, 2014, **5**, 951-958.
3. Z. Liu, R. Ma, M. Osada, N. Iyi, Y. Ebina, K. Takada and T. Sasaki, *J. Am. Chem. Soc.*, 2006, **128**, 4872-4880.
4. C. Chen, P. Gunawan, X. W. D. Lou and R. Xu, *Adv. Func. Mater.*, 2012, **22**, 780-787; J.-H. Choy, S.-Y. Kwak, Y.-J. Jeong and J.-S. Park, *Angew. Chem. Int. Ed.*, 2000, **39**, 4041-4045; C. Chen, L. K. Yee, H. Gong, Y. Zhang and R. Xu, *Nanoscale*, 2013, **5**, 4314-4320.
5. Y. Gao, J. Wu, Q. Wang, C. A. Wilkie and D. O'Hare, *J. Mater. Chem. A*, 2014, **2**, 10996-11016; S. Abedi and M. Abdouss, *Appl. Cat. A*, 2014, **475**, 386-409; Q. Wang, J. P. Undrell, Y. Gao, G. Cai, J.-C. Buffet, C. A. Wilkie and D. O'Hare, *Macromolecules*, 2013, **46**, 6145-6150; Q. Wang, X. Zhang, J. Zhu, Z. Guo and D. O'Hare, *Chem. Commun.*, 2012, **48**, 7450-7452.
6. C. Chen, M. Yang, Q. Wang, J.-C. Buffet and D. O'Hare, *J. Mater. Chem. A*, 2014, **2**, 15102-15110; M. Yang, O. McDermott, J.-C. Buffet and D. O'Hare, *RSC Adv.*, 2014, **4**, 51676-51682.
7. Q. Wang and D. O'Hare, *Chem. Commun.*, 2013, **49**, 6301-6303.
8. M. Shao, F. Ning, Y. Zhao, J. Zhao, M. Wei, D. G. Evans and X. Duan, *Chem. Mater.*, 2012, **24**, 1192-1197.
9. M. Shao, F. Ning, J. Zhao, M. Wei, D. G. Evans and X. Duan, *J. Am. Chem. Soc.*, 2012, **134**, 1071-1077.
10. C. Chen, P. Wang, T.-T. Lim, L. Liu, S. Liu and R. Xu, *J. Mater. Chem. A*, 2013, **1**, 3877-3880.
11. W. Stöber, A. Fink and E. Bohn, *J. Colloid Interface Sci.*, 1968, **26**, 62-69.
12. F. Caruso, H. Lichtenfeld, M. Giersig and H. Möhwald, *J. Am. Chem. Soc.*, 1998, **120**, 8523-8534; P. G. Hartley, I. Larson and P. J. Scales, *Langmuir*, 1997, **13**, 2207-2214.
13. E. Lippmaa, M. Maegi, A. Samoson, G. Engelhardt and A. R. Grimmer, *J. Am. Chem. Soc.*, 1980, **102**, 4889-4893.
14. P. P. Man, M. J. Peltre and D. Barthomeuf, *J. Chem. Soc., Faraday Trans*, 1990, **86**, 1599-1602.
15. P. Wilhelm and D. Stephan, *J. Colloid Interface Sci.*, 2006, **293**, 88-92.
16. S. Khodabandeh and M. E. Davis, *Microporous Mater.*, 1997, **9**, 149-160.
17. J. Rocha, M. Del Arco, V. Rives and M. Ulibarri, *J. Mater. Chem.*, 1999, **9**, 2499-2503.
18. K. J. MacKenzie and M. E. Smith, *Multinuclear solid-state nuclear magnetic resonance of inorganic materials*, Elsevier, 2002.